Two-dimensional equilibrium surface roughness for dissociative dimer dynamics

Deok-Sun Lee[1,2] and Marcel den Nijs[1]

[1]*Department of Physics, University of Washington, Seattle, Washington 98195*
[2]*School of Physics, Seoul National University, Seoul 151-747, Korea*

Equilibrium crystal surfaces, constrained to equilibrate by means of dissociative dimer deposition and evaporation, have anomalous global surface roughness. We generalize earlier results for one-dimensional interfaces to two dimensions. The global surface width scales with surface size L as $W^2 \sim \ln[L/(\ln L)^{1/4}]$ instead of the conventional form $W^2 \sim \ln L$. The surface roughening transition does not change in nature, but its location is subject to a large and slowly varying logarithmic finite-size-scaling shift.

I. INTRODUCTION

Every now and then a new direction of research sheds an unexpected light on an older topic. In this instance, that older topic is equilibrium surface roughness, and a study of non-equilibrium driven surface growth triggered it. One-dimensional (1D) surfaces lack equilibrium phase transitions, but while being driven their stationary growing states can undergo roughening transitions. A recent example is directed-percolation-type roughening [1]. While generalizing the latter to directed-Ising-type roughening [2,3], Noh *et al.* discovered that the equilibrium point in their phase diagram had unusual properties. The surface width W,

$$W^2(L) = \frac{1}{L} \sum_{\mathbf{r}} \ (\langle h_{\mathbf{r}}^2 \rangle - \langle h_{\mathbf{r}} \rangle^2) \simeq L^{2a}, \qquad (1)$$

did not scale with the conventional (random walk) exponent $\alpha = \frac{1}{2}$ but instead with what seemed to be a value close to $\alpha = \frac{1}{3}$. The origin of this is a global conservation law, an evenness constraint on the occurrences of every surface height, due to the dissociative dimer deposition and evaporation dynamics. They related this to even-visiting random walks (RW) [4], i.e., RW required to visit every site an even number of times. In follow-up studies [5,6], it was shown that the value $\alpha = \frac{1}{3}$ is exact, using a mapping to Lifshitz tails [7] in the density of states of 1D fermions in non-Hermitian random fields.

In this paper we address the issue whether something similar happens in two-dimensional surfaces. We show that the global surface roughness is again anomalous, i.e., that instead of the conventional logarithmic finite-size divergence, $W^2 \sim \ln L$, the width diverges as $W^2 \sim \ln L_{\text{free}}$ with an effective surface size $L_{\text{free}} \sim L/(\ln L)^{1/4}$. Moreover, the surface roughening transition temperature has a large and slowly converging logarithmic finite-size-scaling correction.

The outline of this paper is as follows. In Sec. II we review the most basic version of dissociative dimer dynamics leading to the global evenness constraint. In Sec. III we generalize the 1D results of Noh *et al.* to semi-infinite $N \times L$ lattices and show that the width still scales with $\alpha = \frac{1}{3}$. This involves a representation of the equilibrium surface as a RW inside a N-dimensional tube. In Sec. IV we present our numerical data for a $L \times L$ lattice and generalize the so-called

healing time argument of Noh *et al.* from 1D to 2D. Next, in Sec. V, we map the 2D evenness-constrained equilibrium surface partition function onto that of a 2D surface with annealed random fields that couple to the surface heights, and use this to derive the relation $L_{\text{free}} \sim L/(\ln L)^{1/4}$ analytically. In Sec. VI we discuss the implications of the anomalous roughness to the roughening transition, and in Sec. VII we comment on possible experimental realizations. We summarize our finding in Sec. VIII.

II. DISSOCIATIVE DIMER DYNAMICS

The dynamic process that gives rise to the global evenness constraint has in its bare bone version the following structure. Consider the so-called restricted solid-on-solid (RSOS) model on a 1D or 2D lattice. Every lattice site contains an integer-valued height variable $h_r = 0, \pm 1, \pm 2, ...$, and nearest neighbors can differ only by $\Delta h = 0, \pm 1$. The latter means that only surface steps of height one are allowed. The RSOS model has a long history in the theory of surface roughening transitions (see e.g., Ref. [8]).

Impose now the following dimer-type deposition and evaporation rule on the RSOS model. Particles can arrive on and leave the surface only in pairs (as dimers). Choose at random, two nearest neighbor sites on the lattice. The surface heights of both sites are increased or decreased by one unit (with equal probabilities) but only when those two sites are at equal heights, and when the new configuration would not violate the RSOS rule (only single height steps). This simulates the deposition and the evaporation of horizontal dimers. The dimers are dissociative in the sense that the identity of a dimer is lost after it is deposited, and that a particle can arrive on and leave the surface with a different partner.

This type of dynamics was studied recently in one dimension [2] and it was found that the equilibrium surface width does not scale with $\alpha = \frac{1}{2}$, as in conventional surface dynamics, but with the anomalous exponent $\alpha = \frac{1}{3}$ instead. The value $\alpha = \frac{1}{2}$ is highly generic. Equilibrium long range order cannot exist in 1D and therefore the probability to make an up or down step while walking along an equilibrium surface is uncorrelated beyond a definite correlation length. This implies that the interface width scales similar to the dispersion of a random walker, i.e., $\alpha = \frac{1}{2}$.

Dissociative dimer dynamics circumvents this generic
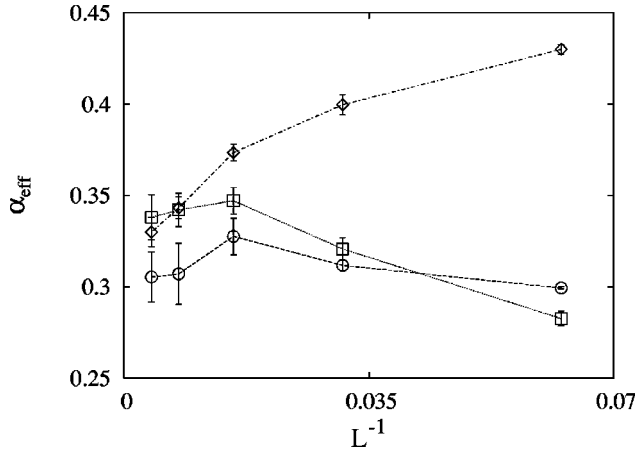
FIG. 1. The effective values of α in Eq. (2) vs the inverse of L are shown for $1 \times L$ surfaces (diamonds), $2 \times L$ surfaces (circles), and $3 \times L$ surfaces (squares) with $L = 16, 32, 64, 128$, and 256.

picture by imposing a nonlocal constraint on the Gibbs distribution. Particles are deposited at each height level in pairs, and therefore the RW must visit each level an even number of times. This is a nonlocal constraint, due to the dissociative character of the dynamics. For example, on a locally flat surface segment, two dimers are able to land next to each other, but next, the two particles in the middle are allowed to switch partners and evaporate together leaving two disconnected monomers behind. Repeated processes such as this leave no local trace of the dimer nature of the dynamics, but globally every height level needs to be occupied an even number of times. In contrast, nondissociative dimer dynamics obeys the constraint locally and therefore yields the conventional scaling exponent $\alpha = \frac{1}{2}$, just as monomer dynamics.

III. SEMI-INFINITE LATTICES

We start with a generalization of the one-dimensional 1 $\times L$ lattice results of Noh *et al.* to $N \times L$ lattices with $N = 2, 3, \dots$. On the one hand, having several channels instead of one weakens the evenness constraint and may be sufficient to alter the $\alpha = \frac{1}{3}$ exponent. On the other hand, critical exponents change typically only with dimension, and these N channel lattices are still 1D systems at large length scales.

Our simulation results are shown in Fig. 1. We plot the effective values of α as functions of the system size L for $N = 2$ and 3, evaluated as

$$\alpha_{\text{eff}}(L) = \frac{\ln[W(L)/W(\frac{1}{2}L)]}{\ln 2}. \quad (2)$$

The roughness exponent remains close to $\alpha = \frac{1}{3}$ for both $N = 2$ and $N = 3$. The convergence is not impressive but comparable to that in the original one channel case. These large finite-size-scaling corrections are explained at the end of this section.

The numerical results for α suggest that we seek an analytical generalization of the even-visiting random walk representation of the system and from that show that the surface

roughness exponent does not indeed change. Consider a walk along the equilibrium $2 \times L$ surface from one edge to the other (from $x = 0$ to $x = L$). The x coordinate plays the role of time and going up or down along the surface is the RW aspect. The walk does not obey the evenness constraint along one specific channel, $y = 1$ or $y = 2$, because dimers can be deposited in two orientations, along and perpendicular to the channel. However, if you walk twice, one time in each channel, then the constraint is still obeyed for the two combined walks. The evenness constraint is weakened, but obviously still present.

On a formal level, the connection between the random walk and surface roughness follows from the well-known transfer-matrix formalism for evaluating the partition function of the surface. Let us first consider a 1D lattice with monomer-type dynamics (no evenness constraint). The labels n and n_0 in the partition function $Z(n|n_0)_x$ represent fixed boundary conditions of the surface at both ends, $h = n_0$ at site 0, and $h = n$ at site x. $Z(n|n_0)_x$ obeys the recursion relation

$$Z(n|n_0)_{x+1} = Z(n|n_0)_x + Z(n-1|n_0)_x + Z(n+1|n_0)_x, \quad (3)$$

which is a discrete version of the diffusion equation and can be reinterpreted as the time evolution of a 1D random walker with $Z(n|n_0)_x$ the unnormalized probability to find the walker at position n at time $t = x$ starting from position n_0 at time $t = 0$.

Let us generalize this to the two channel lattice. n now becomes a two-component vector, $\mathbf{n} = (n_1, n_2)$. The transfer-matrix-type recursion relation

$$Z(n_1, n_2|\mathbf{n}_0)_{x+1} = \sum_{m_1, m_2} Z(n_1 - m_1, n_2 - m_2|\mathbf{n}_0)_{x_1} \quad (4)$$

could be easily solved numerically because the transfer matrix is still finite. However, for the sake of the evenness constraint, we will pursue that Eq. (4) resembles again a diffusion equation and again can be reinterpreted as the time evolution of a RW, but this requires some care and the introduction of an absorbing wall.

This is a walk on a 2D lattice (n_1, n_2). The dimension of the walker's space is equal to the number of channels and not to the dimension of the surface. $h(1, x)$ represents the n_1 coordinate and $h(2, x)$ the n_2 coordinate of the walker at time $t = x$. For example, when the walker is located at site (4, 5) at time $t = 10$, the surface height at site (1, 10) is equal to $h = 4$, and at site (2, 10) equal to $h = 5$.

The integer-valued summation labels m_1 and m_2 in Eq. (4) are subject to the RSOS condition that nearest neighbor surface columns can differ only by $\Delta h = 0, \pm 1$. This translates into two restrictions: First, at every moment in time, the two coordinates of the walker can differ only by $n_2 - n_1 = 0, \pm 1$. So the walk is restricted in the (n_1, n_2) plane to a strip centered along the diagonal, $n_1 = n_2$, as illustrated in Fig. 2. In other words, the walk remains quasi-one-dimensional after all. Second, due to the same RSOS rule, each positional component n_1 and n_2 of the random walk can change only by 0 or ± 1 during each time step, $t = x \rightarrow x$
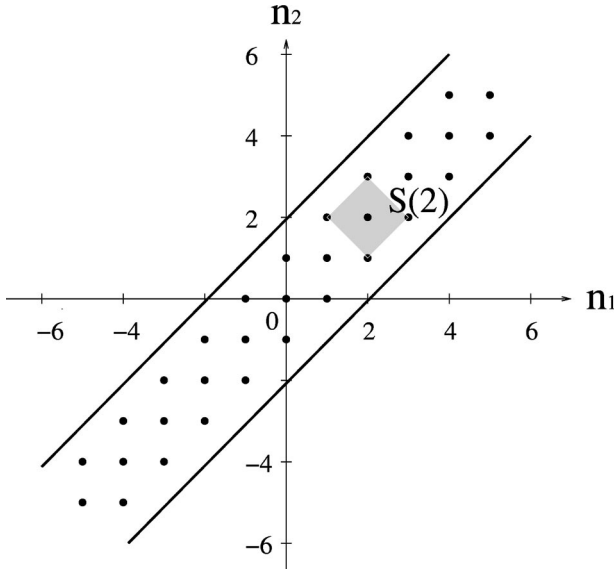
FIG. 2. The $2 \times L$ (2 channel) equilibrium surface representation as a random walk on a strip with absorbing walls. The surface coordinate along the channel represents time in the random walk. The surface heights in the first and second channel represent the n_1 and n_2 coordinates of the walker. The shaded area is an example of a plaquette with Ising spin $S(2) = \pm 1$. The heavy solid lines are the absorbing walls. See the text for more details.

$+1$. It is easy to see that the walker can jump to only six new positions from any diagonal site, $n_1 = n_2$, and to only five from every off-diagonal one, $n_1 \neq n_2$ (in addition to not moving at all).

In the equilibrium Gibbs distributions for the RSOS monomer-type surface dynamics, all surface configurations have equal probabilities. This is reflected in Eq. (4) by the fact that all transition probabilities are equal. However, this recursion relation does not represent yet a proper Master equation for a random walk because it does not conserve probability. A Master equation needs to be of the generic form

$$Z(\mathbf{n}|\mathbf{n}_0)_{t+1} = \sum_{\mathbf{n}'} w(\mathbf{n}',\mathbf{n}) Z(\mathbf{n}'|\mathbf{n}_0)_t, \tag{5}$$

and the transition probabilities, $w(\mathbf{n}',\mathbf{n})$, must conserve probability from any state $\mathbf{n}'$, i.e.,

$$\sum_{\mathbf{n}} w(\mathbf{n}',\mathbf{n}) = 1. \tag{6}$$

The one channel transfer-matrix equation of motion, Eq. (3) is of this form; except that we have to divide all transition probabilities by a common factor, equal to 3. The two channel transfer-matrix equation of motion, Eq. (4) does not satisfy Eq. (6).

Partition functions scale in "time" $t = x$ exponentially as

$$Z(\mathbf{n}|\mathbf{n}_0)_x \sim \lambda_0^x, \tag{7}$$

with λ_0 the largest eigenvalue of their transfer matrices. In Eq. (3), λ_0 is simply equal to 3, i.e., the same common factor that normalizes the transition probabilities. Such a simple common factor does not exist for Eq. (4) because the numbers of sites to which the walker can hop are different at diagonal and off-diagonal sites. This lack of conservation of probability can still be incorporated in the random walk representation by interpreting the boundaries of the strips as so-called absorbing walls. In the absence of the walls, the common factor would have been equal to 3^2. The remaining exponentially decaying factor $(\lambda_0/3^2)^x$ represents the absorption by the walls. Moreover, λ_0^x-type factors drop out of the calculation of thermodynamic averages, which in the random walk representation is equivalent to performing all averages with respect to the so-called surviving ensemble only.

In a free 2D random walk, the fluctuations in the two-components decouple. They do so also in our random walk with absorbing walls on the strip, because we average over the surviving ensemble only. This implies that in the direction parallel to the strip, the root-mean-square displacement scales with the conventional power as

$$\xi_{\parallel}(t) \sim t^{1/2}, \tag{8}$$

at time scales much larger than a characteristic correlation time arising from the range of hopping distances of the RW during each time step. The root-mean-square displacement in the perpendicular direction, $\xi_{\perp}(t)$ remains finite due to the presence of walls. Thus we recover (although in a somewhat contrived manner) the well-known result that for a semi-infinite $2 \times L$ lattice with $L \to \infty$, the equilibrium surface width still scales as in 1D, with $W = [\{\xi_{\parallel}^2(L) + \xi_{\perp}^2(L)\}/2]^{1/2} \sim L^{1/2}$.

Let us return now to the reason for constructing this random walk interpretation, i.e., to deal with the evenness constraint. For the one channel lattice, the core step towards the analytic derivation of $\alpha = \frac{1}{3}$ was the introduction of Ising variables to keep track of where the RW has been before. An Ising spin $S_n = \pm 1$ was associated with each site, and flipped for each time interval the RW resided on that site. The evenness constraint was enforced by requiring that at time $t = x$ all spins point in the same direction as at time $t = 0$. We need only to establish a generalized equivalent formulation to demonstrate that the surface roughness exponent retains its 1D value $\alpha = \frac{1}{3}$ on the two channel lattice.

Introduce an Ising spin $S(n) = \pm 1$ to each diagonal site (n,n), and associate it with the plaquette consisting of sites $(n-1,n)$, $(n,n+1)$, $(n+1,n)$, $(n,n-1)$, and (n, n) on the strip (shown as the shaded area for $n = 2$ in Fig. 2). This spin is flipped for each unit time interval the walker resides on $(n-1,n)$, $(n,n+1)$, $(n+1,n)$, or $(n,n-1)$. $S(n)$ does not flip when the walker resides on the diagonal site (n, n) because then the number of occurrences of height n increases by an even number, $h(1,x) = h(2,x) = n$. Note that two Ising spins flip when the walker occupies an off-diagonal site, i.e., $S(n)$ and $S(n+1)$ for the site $(n,n+1)$.

In the one channel case, the Ising spins act as gate keepers along the chain, and the RW cannot pass site n without flipping its spin $S(n)$. Similarly, in the two channel case, the

RW moves on the quasi-1D strip and again a line of Ising spins act as gate keepers. Topologically and at large length scales, the situations are equivalent and therefore α must be the same as in 1D.

One detail seems different. On the chain, the walker is unable to pass site n without flipping its spin $S(n)$, while on the strip, it can pass through plaquette n without flipping $S(n)$. That might seem an essential difference, but it is not. A relaxed model where a spin is flipped stochastically when the walker passes, was shown by Noh *et al.* in the context of the purely 1D surface to belong to the same universality class as the deterministic spin flip model. This followed most clearly from the transfer-matrix equivalence to Lifshitz tails in the density of states of 1D fermions in non-Hermitian random fields. The random walker is the fermion and the Ising spins generate the random potential (see Ref. [5] for details).

The generalization to $N \times L$ surfaces is straightforward. The RW moves in a N-dimensional tube (i.e., still remains effectively 1D) and the evenness constraint still requires only a single line of Ising spins positioned along the body diagonal of the tube. Each flips when the walker comes within range; $S(n)$ flips every time any coordinate of the RW position is equal to n. We conclude from the above evenness-constrained RW construction that the roughness exponent must indeed retain its 1D value $\alpha = \frac{1}{3}$ for all finite N.

Let us return to our numerical results. The shapes of the curves in Fig. 1 represent so-called finite-size-scaling corrections. These corrections are larger and more complex than for the purely 1D one channel lattice [2]. This can be understood qualitatively as follows. For $N = 1$, the evenness constraint is ineffective at small L such that α_{eff} [see Eq. (2)] decreases monotonically from a value near the free unconstrained RW exponent $\alpha = \frac{1}{2}$ at small L towards $\alpha = \frac{1}{3}$ at $L \to \infty$. [A characteristic crossover system size L could be constructed in terms of the ratio between L and length scale $L_{\text{free}}(L)$ over which the surface fluctuations are unimpeded by the evenness constraint; $L_{\text{free}}(L)$ is defined in the healing time argument of Sec. IV.]

In contrast, the $N = 2$ and $N = 3$ curves start off from a value near 0, overshoot $\alpha = \frac{1}{3}$, and then bend backwards. At small $L < N$, the surface behaves as if it is 2D and as if the evenness constraint is absent, i.e., $W \sim (\ln L)^{1/2}$. This explains why the curves start off at $\alpha \simeq 0$. The surface starts to behave one dimensional beyond $L \sim N$, but initially remains still unaware of the evenness constraint, such that the α curves in Fig. 1 overshoot (towards $\alpha \simeq \frac{1}{2}$) and only back over at larger L where the evenness constraint kicks in.

IV. ROUGHNESS ON $L \times L$ LATTICES

We now turn our attention to dissociative dimer dynamics on a truly 2D $L \times L$ lattice. For monomer-type dynamics, it is well known that the height-height correlation function diverges logarithmically,

$$g(\mathbf{r}) = \langle (h_{\mathbf{r}+\mathbf{r}_0} - h_{\mathbf{r}_0})^2 \rangle \simeq \frac{1}{\pi K_G} \ln r, \qquad (9)$$

and the surface width scales as
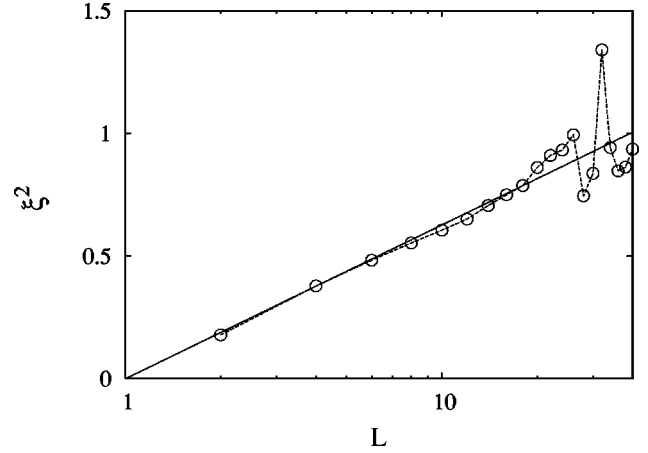
FIG. 3. Semilog plot of the mean-square displacement $\xi^2(L)$ of the random walk in the tube described in Sec. IV as a function of time L for $2 \leq L \leq 40$ with the total random walk time L equal to the dimension of the tubular random walk space N. The solid line fits the form $\xi^2(L) = 0.272 \ln L$ as predicted by Eq. (11).

$$W^2(L) \simeq \frac{1}{2\pi K_G} \ln L, \qquad (10)$$

with K_G the so-called effective Gaussian coupling constant that in the RSOS model at $T \to \infty$ (our numerical simulations) takes the specific value $K_G \simeq 0.9$ [8]. The goal is to find out how the evenness constraint affects this on a global scale.

In the random walk representation of the preceding section, we need to take the limit where the dimension of the tube (N) and the random walk time (L) diverge simultaneously, as $N = L \to \infty$. This diminishes the usefulness of the RW representation. For example, according to Eq. (10), the root-mean-square displacement of the RW along the body diagonal of the tube must scale (for monomer dynamics) as

$$\xi_{\parallel}(L) \sim (L \ln L)^{1/2}. \qquad (11)$$

This might seem at odds with the canonical $\sqrt{L}$ power implied by the RW interpretation; but only until one remembers that the walk is truly random only at time scales L much larger than a characteristic correlation time arising from the maximum hopping distance of the walker during each time step, and realizes that the latter (projected along the tube's body diagonal) is proportional to $\sqrt{N}$, and thus diverges simultaneously with L. For the sake of curiosity, we checked and confirmed Eq. (11) numerically. Figure 3 shows the average root-mean-square displacement, $\xi(L) = [\{\xi_{\parallel}^2(L) + \xi_{\perp}^2(L)\}/L]^{1/2}$ of the RW as a function of $L = N$.

Before we present our numerical results for the evenness-constrained surface width in 2D, we like to present an educated guess of what the behavior might be by generalizing the so-called healing length argument of Noh *et al.* [2] from 1D to 2D. This argument was the least rigorous of their analytical results, but explained the anomalous exponent $\alpha = \frac{1}{3}$ at a simple intuitive level. In 1D and also for all our semi-infinite $N \times L$ surfaces of the preceding section, the argument runs (in a somewhat modified form) as follows.

Consider the semi-infinite $N \times L$ surface. There must exist a crossover length scale L_{free} larger than the surface width N but much smaller than the total channel length L, within which the evenness constraint can be ignored and the surface fluctuates freely such that the surface width increases as

$$W(L_{\text{free}}) \sim L_{\text{free}}^{1/2}, \tag{12}$$

just as in 1D monomer dynamics. The basic premise of the healing length argument is that at larger length scales the surface must be preoccupied satisfying the evenness constraint such that the surface width does not increase any further. Then, we need only to find out how L_{free} scales with L.

Divide the surface strip $0 < x < L$ into segments of length L_{free}. Choose one of these segments and mark all surface heights that are visited an odd number of times in that segment. It is known that these defect surface heights are uniformly distributed within the range $|h| < O(W)$ such that their number is also proportional to W [5]. Suppose that the surface compensates for these defects one-by-one along the rest of the strip (ignoring that the additional surface fluctuations introduce new defects as well as repair, simultaneously, other old ones). The average root-mean-square distance the surface must fluctuate vertically to reach that specific defect height is again proportional to W, and that requires a typical horizontal length interval $\Delta x \sim L_{\text{free}}$. So every segment of length L_{free} leads to only one repair on average. Since there need to be W of them, it follows that

$$\frac{L}{L_{\text{free}}} \sim W, \tag{13}$$

and, using Eq. (12), that

$$L \sim W W^2 \quad \text{and} \quad W \sim L^{1/3}, \tag{14}$$

such that for all $N \times L$ lattices the roughness exponent is equal to $\alpha = \frac{1}{3}$.

For the generalization of this argument to $L \times L$ lattices, we divide the 2D lattice in blocks of size $L_{\text{free}} \times L_{\text{free}}$. Within each block the surface fluctuates as if the global evenness constraint does not exist, and the surface width scales as $W^2 \sim (2\pi K_G)^{-1} \ln L_{\text{free}}$. Assume that oddly visited surface heights are uniformly distributed just as in 1D and therefore that their number is proportional to W. The same repairing scheme as above predicts again one repair on average per block, i.e.,

$$\left(\frac{L}{L_{\text{free}}}\right)^2 \sim W, \tag{15}$$

and therefore

$$L \sim W^{1/2} e^{2\pi K_G W^2}. \tag{16}$$

In the limit of large L, we can invert Eq. (16) to

$$W^2(L) \sim \frac{1}{2\pi K_G} \ln\left[\frac{L}{(\ln L)^{1/4}}\right]. \tag{17}$$
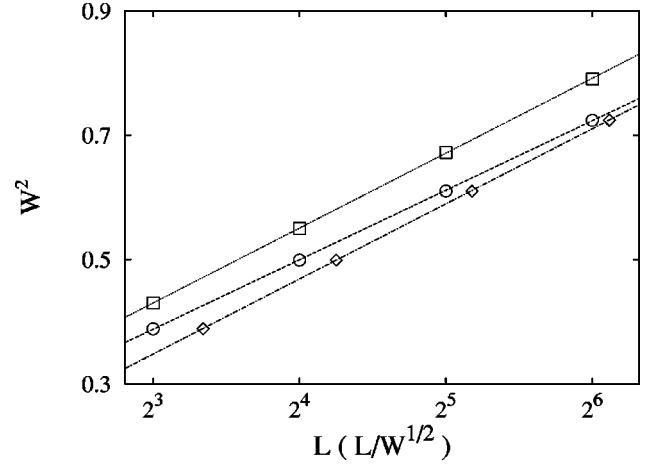
FIG. 4. Semilog plots of equilibrium surface widths W^2 on $L \times L$ lattices for monomer dynamics (squares) and dissociative dimer dynamics (circles) both as functions of L. The slopes of the straight-line fits yield the values of K_G [defined in Eq. (10)]: $K_G = 0.916$ (monomer) and 0.988 (dimer). The diamonds show the same dimer dynamics data plotted as W^2 vs $L/W^{1/2}$. That line has nearly the same slope as that with the squares (monomer dynamics), i.e., $K_G = 0.914$ in agreement with Eq. (17).

The crucial features are the logarithms and the 1/4 power. The former originate from the logarithmic divergence of unconstrained surface roughness in 2D and the latter from the scaling of the number of blocks, $(L/L_{\text{free}})^D$, with dimension D.

Compared to the conventional logarithmic divergence, Eq. (10), the lattice size L is replaced by a logarithmically modified effective length, $L_{\text{free}} \sim L/(\ln L)^{1/4}$. Logarithmic effects are notoriously difficult to confirm numerically, except when you expect them.

In Fig. 4, we present our numerical simulation results. The equilibrium surface width W^2 for monomer and dimer dynamics are plotted on semi-log scales as functions of system size L for $L = 8$, 16, 32, and 64 (squares and circles, respectively). The slope of the monomer curve confirms the value $K_G \simeq 0.9$ of Eq. (10). The dimer roughness line is also quite linear, but with a reduced slope, which means that its surface roughness could be fitted (in this range of length scales) by a simple logarithm, but with an enhanced effective K_G. However, when we plot W^2 versus $L/W^{1/2}$ as suggested by Eqs. (16) and (17), the slope of the (again straight) line is the same as in the monomer case, i.e., we regain the correct value of K_G. Therefore, we conclude that for dissociative dimer dynamics, Eqs. (16) and (17) are indeed correct. In the next section, we put this result on a more rigorous analytic footing.

V. SURFACE ROUGHNESS IN RANDOM MEDIA

Solid-on-solid models come in several variations. The RSOS model we used above, where nearest neighbor columns can differ only by $\Delta h = 0, \pm 1$, is the most convenient for numerical simulations. The so-called discrete Gaussian model [9,10], where the Δh restriction is relaxed and replaced by a Gaussian interaction energy

$$A[h_{\mathbf{r}}] = \frac{E}{k_B T} = \frac{1}{2} K \sum_{\langle \mathbf{r}, \mathbf{r}' \rangle} (h_{\mathbf{r}} - h_{\mathbf{r}'})^2, \qquad (18)$$

between nearest neighbor columns, $h_{\mathbf{r}}$ and $h_{\mathbf{r}'}$ (the meaning of the $\langle \rangle$ brackets in the summation), is more appealing in analytical discussions. In this section we use the latter.

The global evenness constraint can be incorporated in the partition function in the following manner. Define integer-valued variables v_h, one for every surface height. Notice that they are not associated with any specific lattice site. Each v_h is equal to the number of times surface height level h appears in the specific configuration. The partition function, subject to the global evenness constraint, can be written as

$$\mathcal{Z} = \sum_{\{h_{\mathbf{r}}\}} \left[\prod_h \frac{1}{2} (1 + z^{v_h}) \right] \exp(-A[h_{\mathbf{r}}]), \qquad (19)$$

with fugacity $z = -1$. Every configuration in which any of the v_h's is odd receives zero weight.

Next, we introduce randomness degrees of freedom $c_h = 0, 1$ associated with those same surface height levels and write the partition function as

$$\mathcal{Z} = \sum_{\{c, h\}} \exp \left[-\sum_h (\mu c_h v_h + \ln 2) - A[h_{\mathbf{r}}] \right], \qquad (20)$$

with $z = \exp(-\mu)$. Equation (20) can be interpreted as the partition function of an equilibrium surface in the presence of annealed random external fields $\{c_h\}$ that suppress the occurrences of specific surface heights. The noise is global in the sense that the random variable c_h affects surface height level h equally at every position $\mathbf{r}$ along the surface. For every occurrence of height level h, the Boltzmann weight is multiplied by a factor z when $c_h = 1$ (and not if $c_h = 0$). The fugacity parameter z allows us to interpolate between mono-mer and dimer dynamics because at $z = 1$ we retrieve the conventional discrete Gaussian partition function.

We are following in this closely the analogous formula-tion for the 1D surface by Noh *et al.* [5]. They found that in 1D $z = 0$ acts as a special point, a stable fixed point in the sense of renormalization transformations with all $-1 \leq z < 1$ as its basin of attraction. We will show that this remains true in 2D.

The limit $z = 0$ is special. The fugacity Boltzmann factors become δ functions, $z^{c_h v_h} \to \delta(c_h v_h)$, such that the surface is strictly prohibited to pass through all height levels for which $c_h = 1$. Each of them acts as an impenetrable barrier and the surface is restricted in its vertical height fluctuations to wan-der between two such randomly placed walls. The partition function factorizes and reduces to

$$\mathcal{Z} = \sum_{\xi} P(2\xi) \mathcal{Z}_{\xi}, \qquad (21)$$

where $P(2\xi)$ is the probability of finding two neighboring $c_h = 1$ walls at a distance $\Delta h = 2\xi$ apart. Walls are placed at random with probability $\frac{1}{2}$ such that $P(2\xi) = 2^{-2\xi}$. $\mathcal{Z}_{\xi}$ in Eq.

(21) is the partition function of a surface restricted to fluctu-ate between two such hard walls

$$\mathcal{Z}_{\xi} = \sum_{\{h_{\mathbf{r}}\}} \left[\prod_{\mathbf{r}} \theta(\xi - |h_{\mathbf{r}}|) \right] \exp(-A[h_{\mathbf{r}}]). \qquad (22)$$

The two following modifications cannot affect the large length scale behavior. First, below the equilibrium roughen-ing transition the integer-valued height variables $h_{\mathbf{r}} = 0, \pm 1, \pm 2, ...$, can be approximated by real-valued continuous vari-ables with the coupling constant K renormalized to its Gauss-ian value K_G. This is well known from the theory of con-ventional surface roughening [9–13]. Second, we can replace the hard impenetrable walls by soft ones and approximate $\mathcal{Z}_{\xi}$ by

$$\bar{\mathcal{Z}}_{\xi} = \sum_{\{h_{\mathbf{r}}\}} \delta(\langle h^2 \rangle - \xi^2) \exp(-A[h_{\mathbf{r}}]), \qquad (23)$$

where the trace runs over ordinary configurations of the Gaussian model but restricted to the subset where the root-mean-square surface width in each configuration is equal to ξ. The evaluation of $\bar{\mathcal{Z}}_{\xi}$ is elementary. Compared to the Gaussian partition function, $\mathcal{Z}_0 = \Sigma_{\{h_{\mathbf{r}}\}} \exp(-A[h_{\mathbf{r}}])$, it gains an exponential factor,

$$\bar{\mathcal{Z}}_{\xi} \sim \int dm \sum_{\{h_{\mathbf{r}}\}} \exp \left[-\frac{1}{2} K_G \sum_{\langle \mathbf{r}, \mathbf{r}' \rangle} (h_{\mathbf{r}} - h_{\mathbf{r}'})^2 \right.$$
$$\left. + 2\pi i m \sum_{\mathbf{r}} (h_{\mathbf{r}}^2 - \xi^2) \right]$$
$$\sim \mathcal{Z}_0 \exp[-a_0 L^2 \exp(-4\pi K_G \xi^2)], \qquad (24)$$

where $a_0 = \pi/16$. Finally, the surface width of the annealed ensemble average follows from Eqs. (21) and (24) using the method of steepest descent as

$$W^2 \sim \frac{\sum_{\xi} \xi^2 P(2\xi) \mathcal{Z}_{\xi}}{\sum_{\xi} P(2\xi) \mathcal{Z}_{\xi}}$$

$$\sim \frac{\sum_{\xi} \xi^2 \exp[-2\xi \ln 2 - a_0 L^2 \exp(-4\pi K_G \xi^2)]}{\sum_{\xi} \exp[-2\xi \ln 2 - a_0 L^2 \exp(-4\pi K_G \xi^2)]}$$

$$\sim \frac{1}{2\pi K_G} \ln \left[\frac{L}{(\ln L)^{1/4}} \right]. \qquad (25)$$

This is the same scaling form as proposed in the preceding section from the healing argument, Eq. (17).

The above derivation remains equally valid for small val-ues of z around $z = 0$. There, the surface can tunnel through the walls, but with exponentially small probabilities (propor-tional to the length of the intersection contours) actually re-sembling more closely the soft walls in the above derivation.

At the positive z side, it is intuitively reasonable that $z=1$ (the monomer dynamics point) is the horizon and limiting point for this type of scaling. At the negative z side, the horizon extends to and apparently includes the point $z=-1$. The numerical results and also the healing argument of the preceding section suggest this. This is also intuitively consistent. Negative values of z imply an imaginary chemical potential and therefore a mix of positive and negative Boltzmann weights that cancel out against each other; this enhances the exponentially decaying nature of the $|z|^{v_h c_h}$ weight factors, and preserves this decay even at $z=-1$.

VI. ROUGHENING TRANSITIONS

The surface is presumed to be above the roughening transition temperature T_R in most of the above discussion. For example, although Eqs. (19) and (20) apply to all T, it is correct to approximate the discrete Gaussian height variables by continuous Gaussian ones only for $T>T_R$. Everywhere in the rough phase the global surface roughness has a logarithmic correction, Eq. (17), to its conventional simple logarithm. The natural question arises whether and/or how this influences the nature of the surface roughening phase transition. In this section we will show that the evenness constraint has no effect on the properties of the roughening transition in the thermodynamic limit, but gives rise to strong finite-size-scaling corrections, including an apparent shift in the transition temperature.

Equilibrium surface roughness has been a topic of active research over several decades. The roughening is an example of a Kosterlitz-Thouless (KT) transition [14]. Experimental realizations include helium crystal surfaces [15], metal surfaces [16], and organic crystals [17].

The anomalous roughness exists only at a global scale. Within the crossover length scale $L_{\text{free}} \sim L/(\ln L)^{1/4}$ (defined in Sec. IV), the surface fluctuates freely in disregard of the global evenness constraint; i.e., inside the bulk the equilibrium surface remains indistinguishable from that in monomer dynamics, and since phase transitions are ruled by the bulk, the roughening transition must remain in the KT universality class.

The "evenness boundary effect" is, however, very strong. We will approach this from the perspective of the original argument by KT where they estimated the transition temperature by the free energy of a single vortex in, e.g., superfluid films [14]. The discreteness of the height variables, $h_{\mathbf{r}} = 0, \pm 1, \pm 2, ...,$ in the discrete Gaussian solid-on-solid model plays the same role as those vortices. This might be somewhat surprising, but follows mathematically from a so-called duality transformation [11]. In the rough phase, the heights can be treated as continuous variables and this represents the "vortex-free phase." Consider the so-called sine-Gordon correlation function in the Gaussian model, in which the $h_{\mathbf{r}}$'s are continuous,

$$\langle \exp[2\pi i(h_{\mathbf{r}+\mathbf{r}_0} - h_{\mathbf{r}_0})]\rangle = \exp[-\tfrac{1}{2}(2\pi)^2 g(\mathbf{r})] \sim r^{-2\pi/K_G}, \tag{26}$$

[see also Eq. (9)]. The logarithm of this is the free energy of placing two topological objects, $\exp(\pm 2\pi i h)$, at a distance r

apart. They favor integer values of h. That free energy scales logarithmically with distance r, and a single one costs, therefore, an amount of free energy $f=(\pi/K_G)\ln L$ or $f=(\pi/K_G-2)\ln L$ if we allow it to be at any position in 2D space. The temperature $K_G = \pi/2$ where the latter is equal to zero is the famous KT estimate for the transition temperature. (Recall that the coupling constant K_G is measured in units of $k_B T$ such that $K_G \sim T^{-1}$). This is how this works for monomer dynamics.

For dimer dynamics the two sine-Gordon "charges" interact logarithmically, just as in Eq. (26) but only at distances smaller than L_{free}. Closer to the lattice size the interaction levels off such that a single excitation now costs

$$f \simeq \frac{\pi}{K_G} \ln L_{\text{free}} - 2 \ln L. \tag{27}$$

This yields, by setting $f=0$ and using Eq. (17),

$$K_G \simeq \frac{1}{2}\pi \left[1 - \frac{b_0 + \ln(\ln L)^{1/4}}{\ln L} \right], \tag{28}$$

with b_0 a constant. This is a significant finite-size-scaling correction, both in magnitude and in the slowness with which it scales with L. The transition appears to happen at a higher temperature. For example, at $L=1000$ (larger than most experimental surface heterogeneity lengths [16]), the shift is of order

$$\frac{\Delta T_R}{T_R} \simeq \frac{\ln(\ln L)^{1/4}}{\ln L} \approx 7\%. \tag{29}$$

VII. EXPERIMENTAL REALIZATIONS

The scope of this paper is foremost theoretical, i.e., to show how a seemingly benign topological conservation law in the dynamics strongly affects the equilibrium state. Experimental realizations of the evenness constraint should be possible to establish, but this requires careful considerations and collaborations with experimentalists. For example, molecular-type bonded molecules such as N_2 look promising, but unfortunately, in solid N_2 the molecules do not dissociate. As a starting point we include here a section with a brief discussion of the most essential features.

Simple models such as ours are meant and perfectly suited to discover fundamental scaling laws associated with surface growth, but they are rather simple minded when it comes to making direct contact with actual experiments. Those detailed theories of crystal growth have reached a high level of sophistication in recent years [18]. The evenness effect represents a topological feature that will be preserved with increased realism. After identifying a suitable experimental system, the evenness constraint needs to be embedded into the appropriate more detailed theoretical description. However, at this stage, it suffices to focus on general aspects, in particular those that possibly upset the conservation law.

The condition in our model that the X_2 molecules land only horizontally is not a serious constraint, because the mol-

ecule must dissociate as well. The latter requires that the binding energy between the two atoms be weaker or at best be of the same order of magnitude as the bonding energies inside the solid. In that case, both atoms strongly prefer to be close to the surface, and a vertically landed molecule will quickly decay.

A more serious issue is surface diffusion, which is omitted in our model. The evenness constraint is preserved as long as a surface wanders around on the same terrace, but is lost when surface atoms jump across steps to lower or higher levels. Diffusion across steps is reduced by the presence of so-called Schwoebel barriers [19]. If those barriers are strong enough, the jumps will occur infrequently enough that the evenness constraint remains satisfied at length scales large compared to the heterogeneity length scale of the experimental surface. The latter is the length scale at which defects such as impurities pin and limit the surface dynamics; this length rarely exceeds 1000 Å.

Moreover, recall that the anomalous surface roughness is stable with respect to a variation in the fugacity parameter z in Eq. (19), i.e., it remains present when the evenness constraint is not strictly obeyed but only statistically. Therefore it might well be that diffusion across steps preserves the anomalous roughness beyond the above estimate. This issue needs further theoretical study.

Finally, the search for experimental realizations need not be limited to dimer-type dynamics. The anomalous global surface roughness exists and is the same for X_n-type dissociative dynamics with any $n > 1$. This was found to be true earlier in 1D [5], and follows also in 2D from generalizing our analytic arguments.

VIII. SUMMARY

In this paper we studied how equilibrium surface roughness in two-dimensional surfaces is affected by a global constraint that every surface height be present an even number of times in every configuration. We presented numerical and analytic evidences.

In semi-infinite $N \times L$ surfaces, the evenness constraint is weakened compared to the $1 \times L$ surface, but not enough to change the global width. It still scales anomalously as $W \sim L^{1/3}$, just as in purely 1D surfaces [2,5].

In truly 2D $L \times L$ surfaces, the global surface roughness is also anomalous, but the effect is weaker. The surface width scales logarithmically as

$$W^2(L) \sim \ln L_{\text{free}}, \tag{30}$$

similar to conventional monomer dynamics, but with a logarithmically corrected effective surface size

$$L_{\text{free}} \sim \frac{L}{(\ln L)^{1/4}}. \tag{31}$$

The surface roughening transition does not change in nature, but its location is subject to a large and slowly varying logarithmic finite-size-scaling shift, Eq. (29).

These results remain valid when the evenness constraint is only statistically obeyed. Moreover, the analytic derivation in Sec. V involves a mapping onto a surface model with annealed randomly placed barriers, placed horizontally to the surface, that inhibit the vertical surface fluctuations. The surface roughness of those surfaces behaves the same as the evenness constrained ones.

Finally, 2D represents a critical dimension for ordinary equilibrium surface roughness. This follows trivially by evaluating the surface roughness in the Gaussian approximation, $W \sim L^\alpha$, with $\alpha = (2 - D)/2$ (logarithmic in $D = 2$). The surface width does not diverge in dimensions $D > 2$ and the surface remains asymptotically flat. Still, the healing length and random field arguments can be generalized to higher dimensions: $L_{\text{free}} \sim L^{[2D/(2+D)]}$ and $W \sim (L_{\text{free}})^\alpha \sim L^{D(2-D)/(2+D)}$. So, for example, in $D = 3$, monomer dynamics yields $W \sim L^{-1/2}$ and dissociative dimer dynamics $W \sim L^{-3/5}$. The evenness constraint always flattens the surface at a global scale.

[1] U. Alon, M. R. Evans, H. Hinrichsen, and D. Mukamel, Phys. Rev. Lett. **76**, 2746 (1996).

[2] J. D. Noh, Hyunggyu Park, and M. den Nijs, Phys. Rev. Lett. **84**, 3891 (2000).

[3] H. Hinrichsen and G. Ódor, Phys. Rev. Lett. **82**, 1205 (1999).

[4] G. M. Cicuta and M. Contedini, e-print math.PR/9903063; G. M. Cicuta, M. Contedini, and L. Molinari, J. Stat. Phys. **98**, 685 (2000).

[5] J. D. Noh, Hyunggyu Park, Doochul Kim, and M. den Nijs, Phys. Rev. E **64**, 046131 (2001).

[6] M. Bauer, D. Bernard, and J. M. Luck, J. Phys. A **34**, 2659 (2001).

[7] R. Friedberg and J. M. Luttinger, Phys. Rev. B **12**, 4460 (1975).

[8] M. den Nijs, J. Phys. A **18**, L549 (1985).

[9] S. T. Chui and J. D. Weeks, Phys. Rev. B **14**, 4978 (1976).

[10] J. V. José, L. P. Kadanoff, S. Kirkpatrick, and D. R. Nelson, Phys. Rev. B **16**, 1217 (1977).

[11] H. J. F. Knops, Phys. Rev. Lett. **39**, 766 (1977).

[12] For reviews on the theory of surface roughness, see e.g., J. D. Weeks, in *Ordering in Strongly Fluctuating Condensed Matter Systems*, edited by T. Riste (Plenum, New York, 1980), p. 293; H. van Beijeren and I. Nolden, in *Structures and Dynamics of Surfaces*, edited by W. Schommers and P. von Blanckenhagen (Springer, Berlin, 1987); M. Wortis, in *Chemistry and Physics of Solid Surfaces VII*, edited by R. Vanselow and R. F. Howe (Springer, Berlin, 1988).

[13] M. den Nijs, in *The Chemical Physics of Solid Surfaces*, edited by D. King and D. P. Woodruff (Elsevier, Amsterdam, 1994), Vol. 7, Chap. 4.

[14] J. M. Kosterlitz and D. J. Thouless, J. Phys. C **6**, 1181 (1973); J. M. Kosterlitz, *ibid.* **7**, 1046 (1974).

[15] P. E. Wolf, F. Gallet, S. Balibar, and E. Rolley, J. Phys. (France) **46**, 198 (1985); Y. Carmi, S. G. Lipson, and E. Polturak, Phys. Rev. B **36**, 1894 (1987).

[16] For a set of recent reviews on metal surface properties, see e.g., *The Chemical Physics of Solid Surfaces*, edited by D. King and D. P. Woodruff (Elsevier, Amsterdam, 1994).

[17] See e.g., R. F. P. Grimbergen, H. Meekes, P. Bennema, H. J. F. Knops, and M. den Nijs, Phys. Rev. B **58**, 5258 (1998).

[18] Examples of reviews from the vast literature on epitaxial surface growth. A.-L. Barabási and H. E. Stanley, *Fractal Concepts in Surface Growth* (Cambridge University Press, Cambridge, 1995); T. Halpin-Healy and Y.-C. Zhang, Phys. Rep. **254**, 215 (1995); A. Pimpinelli and J. Villain, *Physics of Crystal Growth* (Cambridge University Press, Cambridge, 1998); J. A. Venables, G. D. Spiller, and M. Hanbucken, Rep. Prog. Phys. **47**, 399 (1984); H. Brune, Surf. Sci. Rep. **31**, 121 (1998).

[19] G. Ehrlich and F. G. Hudda, J. Chem. Phys. **44**, 1039 (1966); R. L. Schwoebel and E. J. Shipsey, J. Appl. Phys. **37**, 3682 (1966).